J. Ind. Geophys. Union (January 2016)
Special Volume-2/ 2016 pp: 87-98

On the role of atmospheric tides in the quiet-time variabilities of equatorial electrojet

S. Gurubaran[1,2], S. Sathishkumar[2] and B. Veenadhari[1]

[1]Indian Institute of Geomagnetism, New Panvel (W), Navi Mumbai, India
[2]Equatorial Geophysical Research Laboratory, Indian Institute of Geomagnetism, Tirunelveli, India,
su.gurubaran@gmail.com

ABSTRACT

Simultaneous observations of geomagnetic field variations and upper mesospheric winds by MF radar from low latitudes spanning over a period of 19 years (1993-2011) are utilized in the present work to assess the role of upper atmospheric tides in causing the long-period variabilities of equatorial electrojet (EEJ). Decomposition of ground magnetic data by adopting the method of natural orthogonal components (MNOC) (also referred to as the Principal Component Analysis (PCA))enables the separation of the normal quiet-time behaviour (the expected diurnal variation) and the abnormal (features like counter electrojet (CEJ)) field variation. Using the second principal component as a proxy for CEJ, we show in this work that the CEJs occur more frequently during the solar minimum years and a high degree of correlation is noticed between the enhanced tides during the solar minimum years and the occurrence of CEJs then.

Keywords: Geomagnetism, Equatorial Ionosphere, Equatorial Electrojet, Atmospheric Tides

INTRODUCTION

Tidal winds generate electric fields and currents in the E region of the ionosphere where the transverse conductivities maximize. The ionospheric current system arising during magnetically quiet times is referred to as the solar-quiet (Sq) current system and has been a subject of interest for several decades. During daytime, the Sq current vortices are characterized by an anticlockwise flow in the Northern Hemisphere and a clockwise flow in the Southern Hemisphere, both moving with the apparent motion of the Sun. The principal driver for the Sq current pattern is the solar first symmetrical evanescent (1,-2) diurnal tide (*Tarpley, 1970b*). Surface geomagnetic field observations can be used to deduce equivalent current distributions concentrated in a thin concentric shell. With such an approach, several studies have been carried out in the past since the early work of Chapman and Bartels (*1940*), delineating the structure of the Sq current system and its time and space variations (e.g., *Matsushita and Maeda, 1965; Matsushita, 1967; Malin and Gupta, 1977; Suzuki, 1979; Campbell et al., 1992; Takeda, 1999*). The ionospheric wind dynamo theory that explains the formation of the Sq current system is well documented in the literature (*Richmond, 1995, and references therein*).

An important element in the study of quiet-time ionospheric current system is its significant day-to-day variability. Modelling of Sq faces the challenge of identifying tidal mode or a combination of tidal modes, driving the worldwide ionospheric current pattern, at any instant, that is in agreement with signatures of an equivalent current distribution obtained from the ground magnetic variations. Earlier studies presumed the diurnal tide to be the dominant driver of the current system. Later modelling efforts incorporated the dynamo effects induced by semidiurnal tides (*Stening, 1977; Richmond et al., 1976; Takeda and Maeda, 1981; Hanuise et al., 1983; Takeda, 1990*, to state a few). However, the disagreement between the simulated effects due to semidiurnal tides and observations persisted, despite significant progress in modelling, (*Richmond, 1995*). Other factors like asymmetric tidal components that might be present during solstices and lunar tidal effects have been invoked to explain the discrepancies between models and observations (*Stening, 1989; Tarpley, 1970a; Stening and Winch, 1979*).

Close to the magnetic dip equator, an intense band of eastward electrical current, the equatorial electrojet (EEJ), flows at a height of ~105 km in daytime within a narrow latitudinal belt (*Onwumechili, 1997, on all aspects of EEJ*). The quiet-time eastward current, on some occasions, reverses its direction and manifests as a negative deviation in the horizontal component of the geomagnetic field (*Mayaud, 1977*). This feature is referred to as reverse or counter electrojet (CEJ). The presence of CEJ at the magnetic equator has been linked to a superposition of an additional current system over the normal Sq (*Bhargava and Sastri, 1977; Stening, 1977b, Marriott et al., 1979; Hanuise et al., 1983; Rastogi, 1994; Alex et al., 1998; Gurubaran, 2002*). After examining several CEJ events and possible wind systems that might be driving them, Stening (*1977b*) concluded that various tidal modes might be able to simulate the observational results. However, to better understand the simulation process knowledge of different wind systems are required on different occasions.

Major unresolved issues in the study of EEJ are: (1) the relationship between the Sq current system and EEJ,

and (2) the causative mechanisms responsible for the quiet-time CEJ phenomenon. In the first, the daily range in the *H*-component of the geomagnetic field at EEJ stations is poorly correlated with the range at low latitudes (*Kane, 1976; Rastogi, 1993; Yamazaki et al., 2010*). It was also hypothesized that the position of the Sq focus would alter the strength of the EEJ (*Tarpley, 1973*) and the correlation improves when this effect is taken into account. The EEJ itself is treated by some authors as a separate current system flowing at lower altitudes and having its own return current at low latitudes (*Onwumechili, 1997*). A strong indication for this is provided by the narrow latitudinal and longitudinal signatures of CEJ. If the global tidal modes are responsible for this reverse current at the equator, the associated changes in the magnetic field elements should occur globally (*Stening, 1977b*). There is a need to explain why tidal modes of global origin do not always produce such changes in Sq pattern globally. An alternate view envisages vertical winds and gravity wave associated shearing winds to be capable of producing such current reversals in narrow latitude and altitude regions (*Raghavarao and Anandarao, 1987*). In a recent work, Yamazaki et al. (*2014b*) revisited the above problem using a whole atmosphere community climate model. The simulation results from this model reveal the irregularity of zonal winds that seems to be responsible for the spatio-temporal variations of EEJ in shorter time scales. Using the Thermosphere-Ionosphere-Electrodynamics-General Circulation Model (TIE-GCM), Yamazaki et al. (2014a) showed that upward propagating tides compete with the in-situ generated tides to take control of the seasonal variabilities of EEJ. When the upward propagating tides are incorporated into the model, they noticed a doubling of the current intensity and the corresponding ground magnetic signature. The model simulations further indicate that the semi-annual variation in EEJ is caused primarily by the semi-annual variation of the upward propagating tides.

The operation of the medium frequency (MF) radar at Tirunelveli (8.7°N, 77.8°E, geographic; 2.2°N magnetic dip) has produced continuous data,since 1992, on winds in the mesosphere-lower thermosphere (MLT) region in the height range 80-98 km (*Rajaram and Gurubaran, 1998*). This offers an excellent opportunity to explore the long- and short-term variabilities in EEJ, which can be explained by similar variabilities in tidal winds in the MLT region. In the present studywe make use of the information on tidal winds retrieved from the MF radar data and the ground magnetometer observations from Tirunelveli (1999 onwards) / Trivandrum (1993-1998), the dip equatorial stations. These stations are under the influence of both Sq and EEJ. In addition we have also made use of the data from Alibag, a station which is located away from the magnetic equator and is under the influence of only Sq. The EEJ strength for every hour is derived from the difference in the horizontal component of the magnetic field between the two stations for that hour. By taking this difference, contributions arising from magnetospheric currents are expected to be minimized.

We utilize the Method of Natural Orthogonal Components (MNOC) (referred to as Principal Component Analysis (PCA) in this work) to decompose the ground magnetic data for the period 1993-2011 and to express the daily variation as a summation of a few eigen modes. It will be demonstrated here in that the first eigen mode of the EEJ represents the fundamental solar driven diurnal component, whereas the second and third eigen modes reveal the presence of higher order solar driven tidal components. When a comparison of the first two eigen modes is made with the MLT tides, we notice several interesting features: the principal or the first eigen mode that also represents the daily range in EEJ reveals solar cycle variability as expected. However, the tides are stronger during the solar minimum years of 2006-2010 and weaker during the solar maximum years of 1999-2002. They are not correlated well with the daily range in EEJ even in the seasonal time scales. Rather, afternoon CEJs are more prominent during solar minimum. Also they appear to be driven by MLT tides.

SELECTION OF DATA AND ANALYSIS

This study utilizes the hourly values of the strength of the EEJ for all months during 1993-2011,when the data on upper mesospheric winds from the MF radar over Tirunelveli are available. It may be recalled that the solar activity was in the descending phase during the initial years of 1993-1995, whereas the activity went through a deep minimum between 2007 and 2010. Days for which there were gaps in the magnetometer data (either for Tirunelveli / Trivandrum or for Alibag) of few hours or more were excluded from the analysis. The number of days for which EEJ data for the full 24 hours are available is then 6705 instead of a possible 6939.

Like in previous work (*Gurubaran, 2002*), we adopt MNOC to separate the normal and abnormal geomagnetic field variations. Several authors have used this technique to unravel a variety of processes that contribute to the observed field components (*Golovkov et al., 1978; Rajaram, 1980, 1983; Xu and Kamide, 2004; Chen et al., 2007; De Michelis et al. 2010,* to state a few). As described in these reports, the procedure involves expanding the observed field in an orthogonal basis and solving the resultant eigen value problem and looking for some simpler patterns. The method is briefly described below.

The hourly geomagnetic field variation is expressed in terms of a set of basic functions called Empirical Orthogonal Functions (Z_{ik}) as:

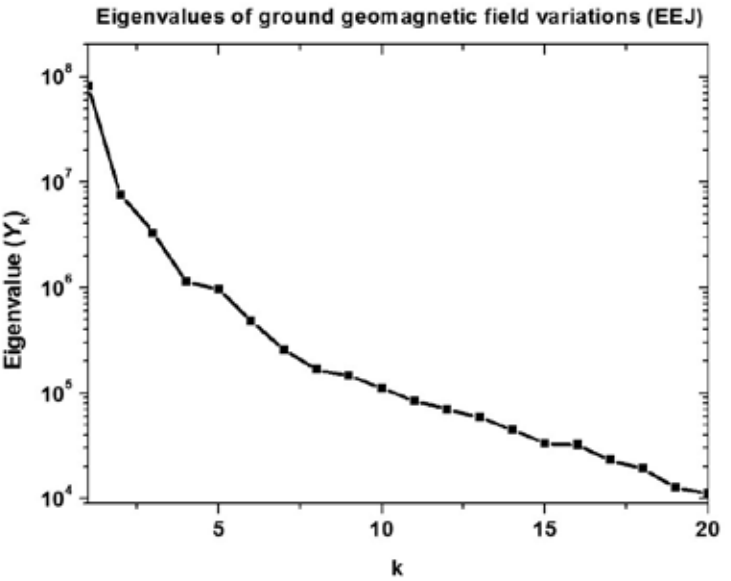

Figure 1. The eigenvalues for the first 20 principal components.

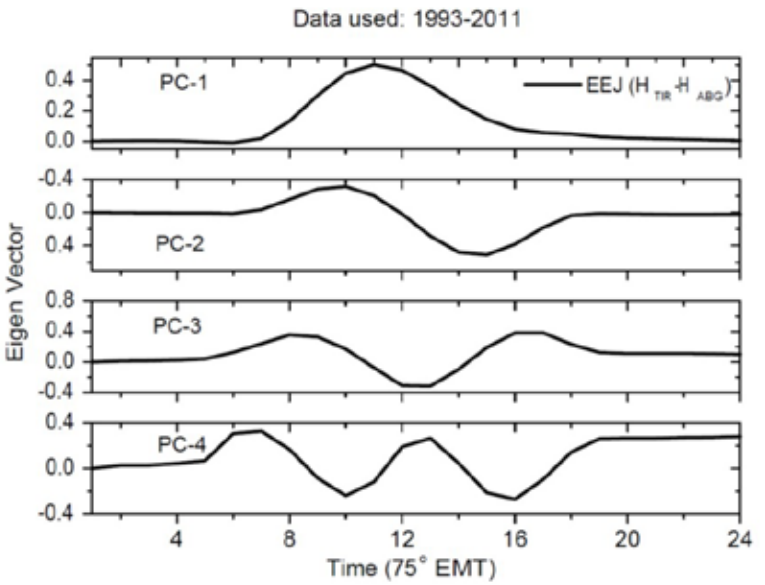

Figure 2. The eigenvectors derived from the MNOC technique.

$$\varphi_{ij} = \sum_{k=1}^{N} h_{ki} Z_{jk} \quad (1)$$

where i = 1,2,..n represents the number of days and j = 1, 2, …24 represents the hour for a given day i. Here k = 1, 2,...and N is the mode number. In short, Z_{jk} is the mode of the kth component (a 24-hour pattern, in our case) and the corresponding principal component (PC) is h_{ki}, which is the amplitude of the mode for the given day i.

If X_{ij} represents the observed hourly variation, we need to minimize the 'error' that might have occurred in the representation of the observed data by the above series expansion:

$$\delta = \sum_{i=1}^{n} \sum_{j=1}^{24} \left[X_{ij} - \sum_{k=1}^{N} h_{ki} Z_{jk} \right]^2 . \quad (2)$$

This reduces to the following eigen value problem:

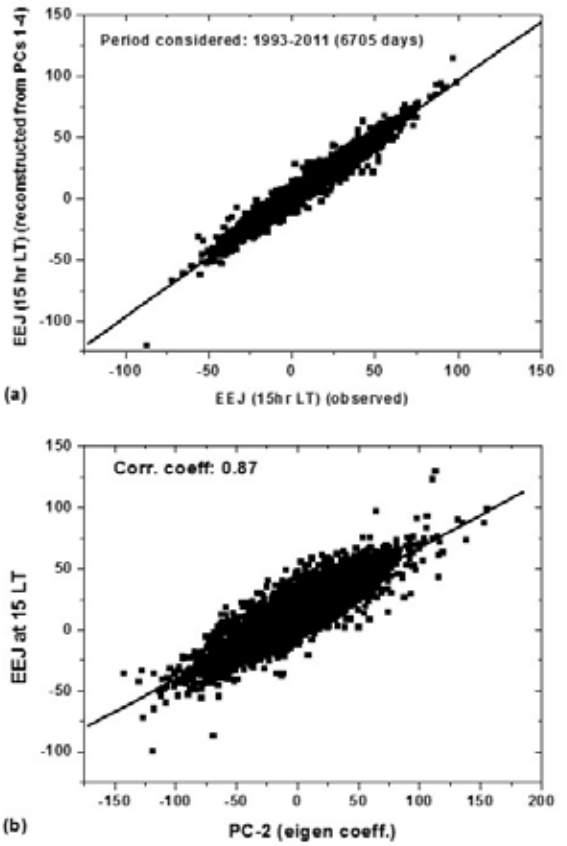

Figure 3. The scatter plots for the observed and reconstructed EEJ strength at 15 LT (top panel) and the PC-2 and EEJ at 15 LT (bottom panel).

$$R_{jk}Z_{jk} = Y_{ki}Z_{jk} \quad (3)$$

where $R_{jk}$is the N x N covariance matrix given by X^TX. Here $X^T$is the transpose matrix.The eigenvalues, Y, and the corresponding eigen vectors, Z, are obtained by solving equation (3).

From equation (1), the amplitudes of the principal components (also referred to as eigen coefficients) for any day, i,can be written as

$$h_{ki} = \sum_{j=1}^{24} \varphi_{ij} Z_{jk}. \quad (4)$$

The eigen values, Y_{ki}, represent a measure of the variance of their corresponding principal components. As we have seen with the large data set chosen for the present work, the observed variation can be explained in terms of the first few eigen modes. Figure 1 reveals the eigen values computed for the first 20 principal components from the EEJ data. The rapid drop of the eigen values is clearly evident. This suggests that the first few eigen modes can almost fully represent the ground geomagnetic field variation.

In Figure 2 we show the results of the PCA for the first four eigen modes. As can be noted, the first eigen mode largely represents the normal quiet day behaviour of EEJ with a maximum around noon hours. Interestingly, the second and third eigen modes reveal features that are characteristic of semidiurnal and terdiurnal components with 12 hour and 8 hour periodicities, respectively. A 6-hour periodicity can be noted in the eigen vector for the fourth PC. As expected, no variation is seen for the night hours (between 18 and 24 and 0 and 6 LT) (time is expressed in local time (LT) or 75°E Meridian Time or in short 75° EMT).

Figure 3a demonstrates how well the first four eigen modes together represent the observed variation field. An excellent comparison has been obtained between the observed and reconstructed EEJ strength for the 15 LT time sector considered for this analysis.

When examined closely, with its characteristic negative minimum around 10 LT and positive maximum around 15 LT, the eigen vector for the second principal component (refer to the second panel from top in Figure 2; also note here that the scale has been reversed) reveals a close relationship with the afternoon CEJ over Tirunelveli (afternoon CEJs are more frequent than morning CEJs). On days of afternoon CEJ, the corresponding eigen coefficient for PC-2 turns out

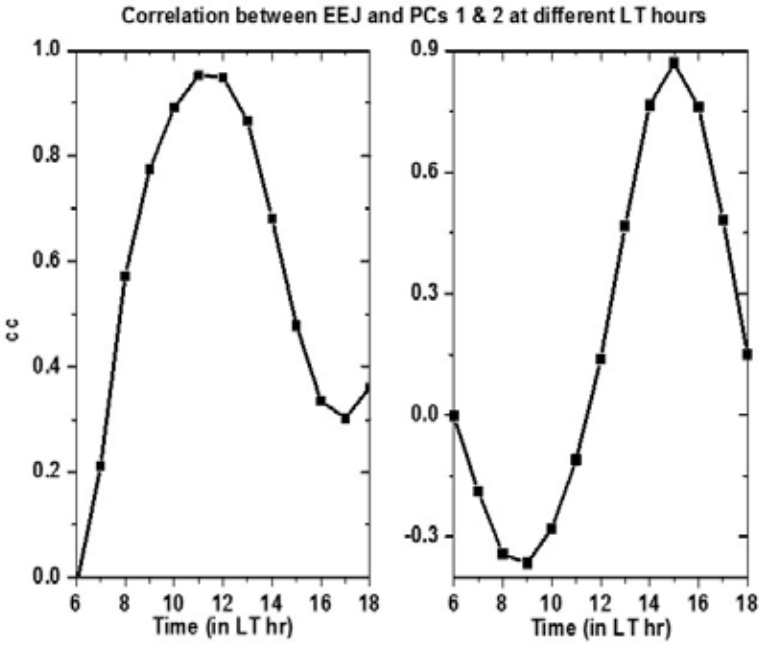

Figure 4. Temporal dependence of the correlation coefficients computed for the EEJ strength at various times and the principal components 1 (left panel) and 2 (right panel).

to be negative accounting for the depression of the EEJ in the afternoon hours (refer to equation (1)). This behaviour of PC-2 is evident in Figure 3b, wherein the EEJ at 15 LT is compared with the PC-2 eigen coefficient in the form of a scatter plot. With a correlation coefficient of 0.87 and PC-2 thus contributing to 76% of the variability, we conclude that the PC-2 eigen coefficient can be used as proxy for the afternoon CEJs that are more spectacular and more frequent than the morning CEJs. The small scatter in Figure 3b is likely due to other modes that could have contributed to the rest of the variability at this time. Earlier, Rajaram (*1980*) had successfully adopted the MNOC technique to decompose the normal and abnormal variations of equatorial geomagnetic field. In that work the first principal component was shown to contain information about Sq and EEJ, whereas the second principal component was closely related to CEJ and disturbance field variations.

Before we present the main results, we compare the daily eigen coefficients of PCs 1 and 2 with the observed EEJ at local times between 06:00 and 18:00 hours (Figure 4). Interestingly, PC-1 eigen coefficient shows the largest correlation coefficient of 0.95 at 11 and 12 LT, whereas PC-2 eigen coefficient reveals a small negative correlation in the morning hours and a greater positive correlation in the afternoon hours. We point out here that the high correlation (~0.95) between EEJ and PC-1 for the noon hours indicates that PC-1 represents well the daily range of EEJ. Largest (~0.9) positive correlation for EEJ and PC-2 in the afternoon hours, when EEJ displays a depression, indicates that the afternoon CEJ can indeed be represented by PC-2. As noted earlier, the PC-2 eigen coefficient does become negative on afternoon CEJ days.

Finally, to appreciate how the PCA works on the EEJ data, we present two examples (Figure 5), one representing the occurrence of CEJ on 14 January 2006 (shown on the left panels) and the other, the normal EEJ on 20 January 2006 (shown on the right panels), both days being magnetically quiet. In a series of panels one below the other, we show how addition of PCs (superposition of various modes) one by one tend to capture the observed EEJ variation. On 20 January 2006, PC-1 (black curve) alone almost reproduces the observed EEJ (red curve) with a large positive value of 228 for the corresponding eigen coefficient. On 14 January 2006, EEJ did not develop at all during daytime. Rather, we notice a large afternoon CEJ event with the depression in observed EEJ reaching up to -95 nT on 14 January 2006. Even with a large negative value of 50 nT, one can see that PC-1 is not able to reproduce the CEJ feature on this day. As expected from the PCA, the second and third PCs enable the CEJ feature appearing between 13 and 14 LT. Interestingly, the signs of the first three eigen coefficients were opposite between the two days: PC-1 and PC-2 eigen coefficients were negative on the CEJ day with values of -104 and -114, respectively, whereas they were positive on the normal day (i.e., on 20 January 2006) with values of 228 and 25, respectively. PC-3 amplitude was positive on the CEJ day and negative on the normal day. When several days were carefully examined,

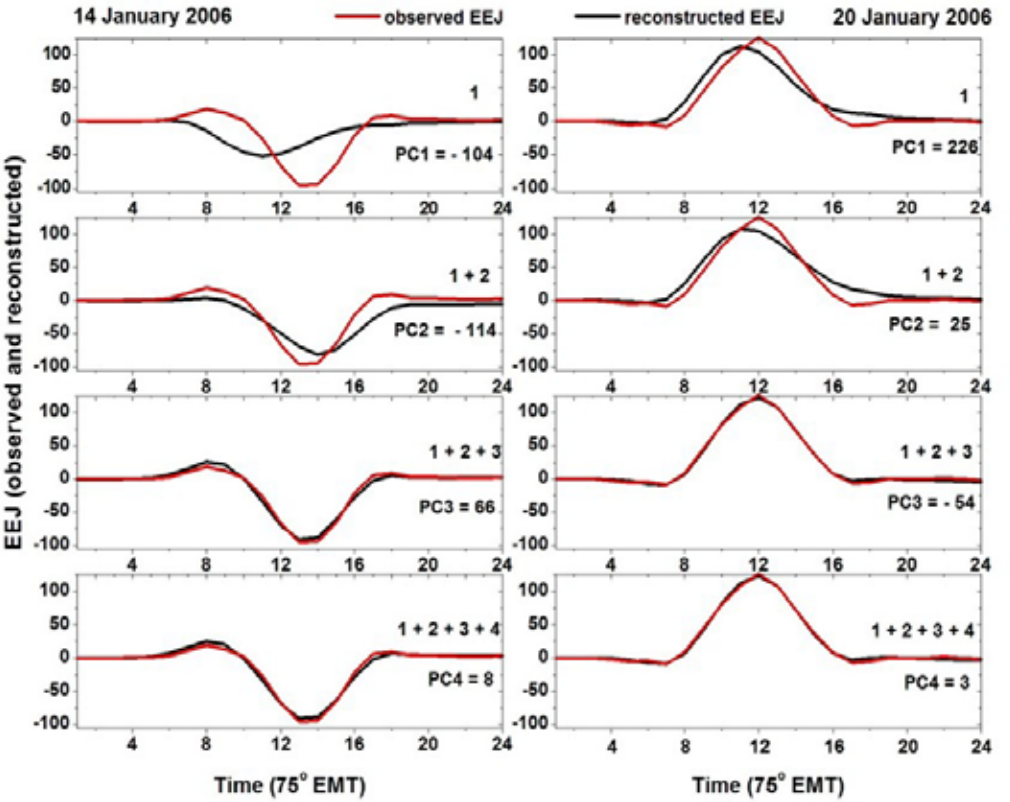

Figure 5. Observed and reconstructed EEJ for 14 January 2006 (left) and 20 January 2006 (right). The observed EEJ is shown as red curves whereas the reconstructed EEJ values are shown as black curves. Increasing number of PCs are used to reconstruct as we slide down from the top (for example, topmost panels were reconstructed from the first PC, second from the top were reconstructed using the first and second PCs together, etc.). The amplitudes of the PCs are also indicated in each panel.

it was noticed that on all CEJ days PC-2 amplitudes were largely negative. Further, the greater the CEJ intensity, the smaller (or more negative) was the PC-2 amplitude.

VARIABILITIES OF EEJ IN SEASONAL AND SOLAR CYCLE TIME SCALES

We begin this exercise by examining the first two principal components (essentially, their eigen coefficients) computed for the EEJ strength. The daily values were averaged in monthly time segments and the results are plotted in Figures 6a and 6b. In this exercise we did not remove the disturbed days. A quick look at these plots exhibits the features expected for the normal EEJ and the abnormal CEJ. The equinoctial maxima and the solstitial minima for the first principal component plotted in Figure 6a, which is a measure of the diurnal range of EEJ,are the regular features. This semiannual pattern is clearly modulated by the solar cycle influence. For example, the largest amplitudes(in the range 150-200) for the first principal component are observed during the solar maximum years of 2000 and 2001. During the solar minimum years of 1995-1997 and 2007-2010, the first principal component was relatively weaker (with its eigen coefficient in the range 80-100),implying that the diurnal range in EEJ was smaller during these years.

As discussed earlier, the second dominant principal component, especially when the corresponding eigen coefficient is negative,reveals the abnormal CEJ or reverse electrojet occurring in the afternoon hours. The monthly averaged eigen coefficient for this principal component plotted in Figure 6b exhibits negative values (reaching up to -40) during summer solstices (May-August) and positive values during other months (except for April). Large negative values over an extended period of time are noticed during the solar minimum years (1995, 2009 and 2010). For these years the CEJ occurrences are 221, 242 and 204, respectively, whereas CEJs during the solar maximum years of 2000 and 2001 are 96 and 121, respectively. The frequent occurrence of afternoon CEJs during the summer months and during solar minimum years is a well known feature for the Indian sector (*Rastogi, 1974; Bhargava et al., 1983*). In the present work, we notice 1593 days of CEJ occurrences during summer and 869 and 888 days of CEJ occurrences during winter and equinox months,

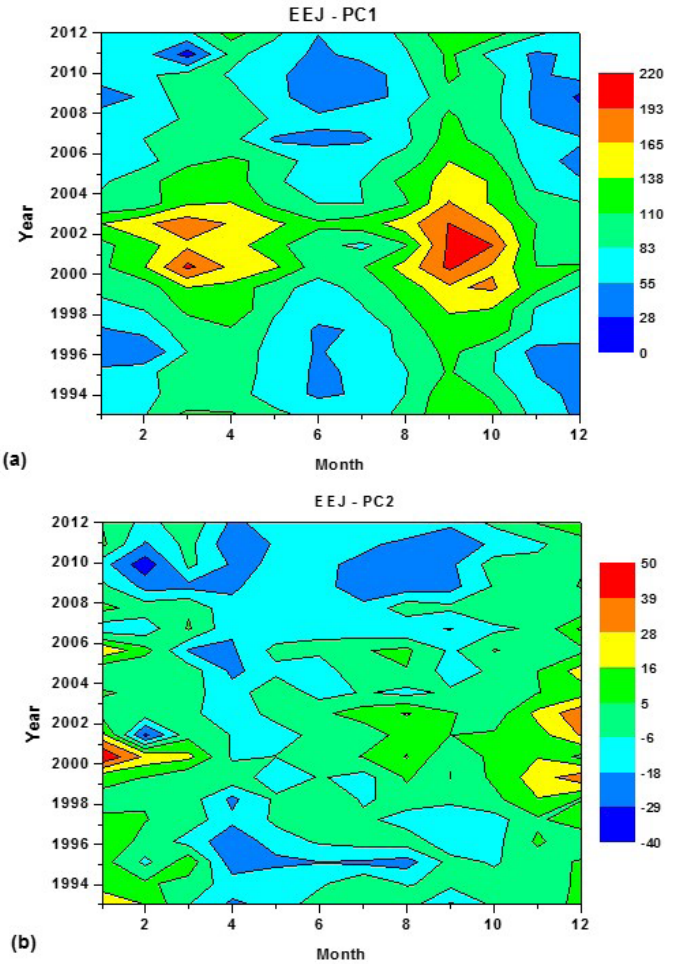

Figure 6. (a) The first principal component of EEJ plotted with season for the years 1993-2011. (b) Same as in (a) but for the second principal component.

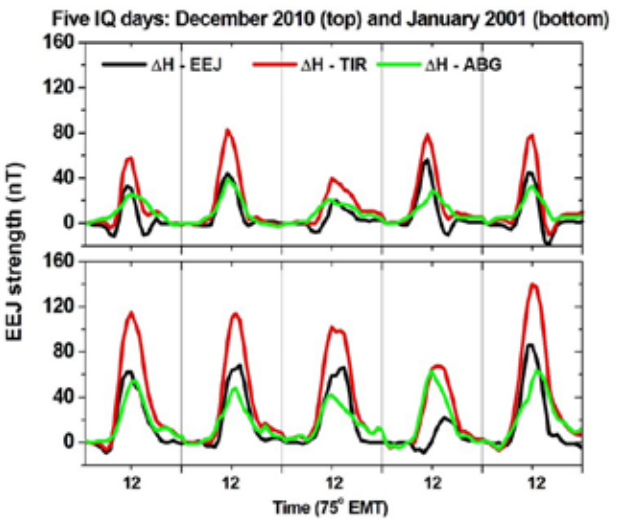

Figure 7. Hourly EEJ strength shown for the internationally classified quiet days during December 2010 (top) and January 2001 (bottom), representing solar minimum and solar maximum years, respectively.

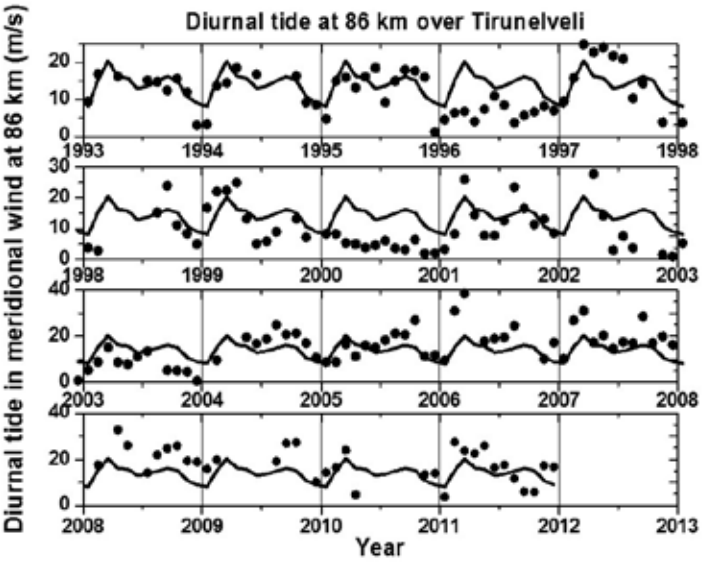

Figure 8. Amplitude of the diurnal tide in meridional wind at 86 km (see text for details).

respectively. With the results from this work agreeing with the previous, on the general behaviour of EEJ and CEJ,one can conclude that the PCA proves to be a valuable tool for assessing the long-term variabilities.

Long-term observations of neutral winds in the mesosphere-lower thermosphere region from Tirunelveli have also helped to examine the role of atmospheric tides in causing the observed variabilities in EEJ in various time scales. Earlier work from this station had shown the links between semidiurnal tides and CEJ during wintertime sudden stratospheric warming (SSW) events (*Sridharan et al., 2009; Sathishkumar and Sridharan, 2013*). During the SSW events that occurred during 1998-1999 and 2005-2006, the semidiurnal tide at 88 km over Tirunelveli was shown to have enhanced amplitudes possibly driving the CEJ events observed during these times (*Sridharan et al., 2009*). The later work by Sathishkumar and Sridharan (*2013*) focused on lunar tides in both mesospheric winds and EEJ during the SSW event of 2008-2009. One of the puzzling aspects of this work has been the enhanced lunar tidal signature in EEJ, whereas the lunar tide in mesospheric winds did not show any enhancement during the SSW.

While carefully examining the diurnal profiles of EEJ, we have noticed the differing nature of the variation during the solar maximum and solar minimum years. In Figure 7 we show the diurnal EEJ curves for the five internationally classified quiet days for December 2010, a solar minimum period (shown in the top panel) and January 2001 (shown in the bottom panel), a solar maximum period. As mentioned earlier, two features can be clearly identified in these curves: (i) Larger diurnal range during January 2001 when compared to December 2010 and (ii) occurrence of afternoon/morning CEJ on four out of five days during 2010.

To better understand the differing nature of EEJ, we have systematically analysed these differences and arrived at more plausibleunderlying causative mechanisms. For this exercise, we have considered tidal amplitudes and phases for the altitude of 86 km by selectively choosing the best radar data acceptance rates. Such a screening and selection has been necessitated as Radar echoes from higher altitudes (92 km and above) are known to be contaminated by EEJ and the radar derived motions are expected to be more closely related to electric fields than to neutral winds at those altitudes (*Gurubaran and Rajaram, 2000*).

In Figure 8 we present the results for the monthly amplitudes of diurnal tide in the meridional wind at 86 km over Tirunelveli for the period 1993-2011. The monthly estimates are shown as symbols, whereas the annual variation in the climatological sense is shown as a thick curve (repeats every year in the figure). One can notice significant deviations of the monthly diurnal tide amplitudes from the climatological mean. During certain years, the tidal activity was greatly enhanced (2007 and 2008, for example),whereas during other years, the monthly tidal amplitudes were smaller than their respective climatological means (1996 and 2000, for example). Especially after 1999, we have noticed a remarkable feature of the upper mesospheric tides over Tirunelveli. The observed strong solar cycle dependence is striking. We have observed presence of larger amplitudes during solar minimum years of 2006-2010 and reduced amplitudes during 1999-2001, when the solar activity was at its peak. Similar solar cycle dependence for the semi-diurnal tide in the wind components at 86 km over Tirunelveli has also

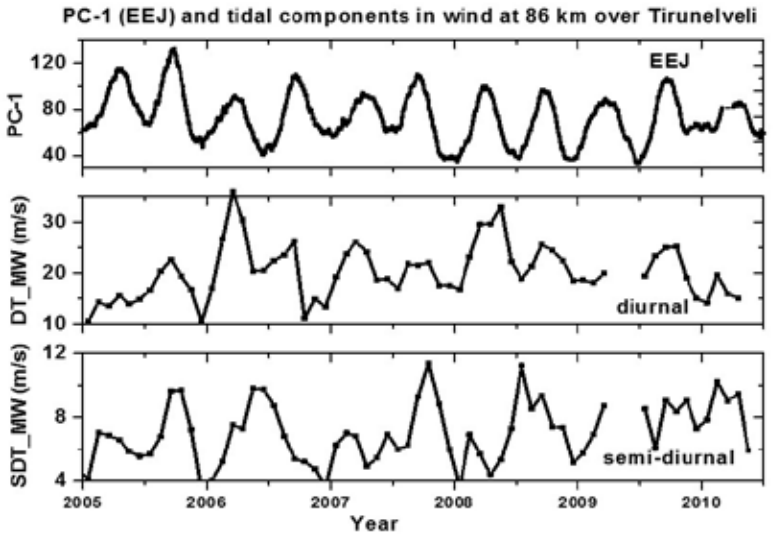

Figure 9. Comparison for the first principal component (top panel) representing the diurnal range in EEJ and the diurnal and semi-diurnal tide components (middle and bottom panels) in wind at 86 km.

been noticed (not shown here). Earlier, Sridharan et al. (*2010*) noted a negative solar cycle response for the tidal amplitudes over Tirunelveli, while using data obtained over a smaller number of years (1993-2007).

We have also noticed a strong solar cycle dependence of PC-1, which is a measure of the diurnal range in EEJ, with larger values during solar maximum and smaller values during solar minimum (Figure 6a and 6b). This feature is essentially caused by the solar cycle variation of ionospheric electrical conductivity. One can argue that this is not caused by the long-term variability in the mesospheric tides observed over Tirunelveli, as the tidal activity has been weaker during the sunspot maximum years of 2000 and 2001 and stronger during the sunspot minimum years of 2008-2010.

Apart from the solar cycle variability, we also noticed a semi-annual variation in PC-1, which is believed to be partly driven by the in-situ generated thermospheric tides and partly by the upward propagating tides of lower atmospheric origin. In a recent work, using the TIE-GCM simulations that utilize lower atmospheric tidal forcing based on TIMED wind and temperature measurements, Yamazaki et al. (*2014a*) asserted that upward propagating tides play a substantial role in causing the seasonal variability of EEJ.

In Figure 9 we show the comparison for the temporal variation of the first principal component of EEJ and the diurnal and semi-diurnal tidal amplitudes of meridional wind at 86 km over Tirunelveli. The data set chosen for this exercise was for the period 2005-2010. This period was chosen because the solar cycle has already declined and the activity was stable and at its minimum. The 60-day running mean of the eigen coefficient for PC-1represents the EEJ signature. This kind of smoothing enables us to identify the semi-annual variation (two peaks in a year) in EEJ with its characteristic equinoctial maxima and solstitial minima. The tidal amplitudes in the meridional wind at upper mesospheric heights do exhibit a semi-annual variation but during certain years (2006 and 2008, in the case of diurnal tide, for example) larger tidal activity seems to overshadow this behaviour. It is to be noted that these larger tidal amplitudes are not accompanied by similar enhanced variationsin EEJ.

We have also examined the long-term variabilities in the second principal component in EEJ, to explain the tidal wind variabilities. Figure 10(a,b) shows the comparison in monthly time scales for PC-2 and the diurnal and semi-diurnal tide amplitudes in meridional wind at 86 km over Tirunelveli. For this exercise, we have used the principal components only for days for which the geomagnetic activity index, Ap, is less than 6. Further, 6-point running means were considered that would smooth out the short term (~a few months) variabilities in both EEJ and tidal parameters. The entire period range is broken into two parts: 1993-2001 plotted in the left panels and 2001-2011 plotted in the right panels.

An important feature that distinctly appears in both the comparison plots shown in Figure 10 is that beginning with the year 1998 the variations in PC-2 and tidal amplitudes in the longer time scales tend to be similar. When the tidal amplitudes during 1999-2001 (peak sunspot activity) were smaller (5-15 m/s for diurnal tide and 4-6 m/s for semi-diurnal tide), the PC-2 eigen coefficient revealed positive values (also noticed earlier in Figure 6b). During sunspot minimum years of 2008-2010, when the tidal activity was enhanced (the amplitudes were greater up to two times

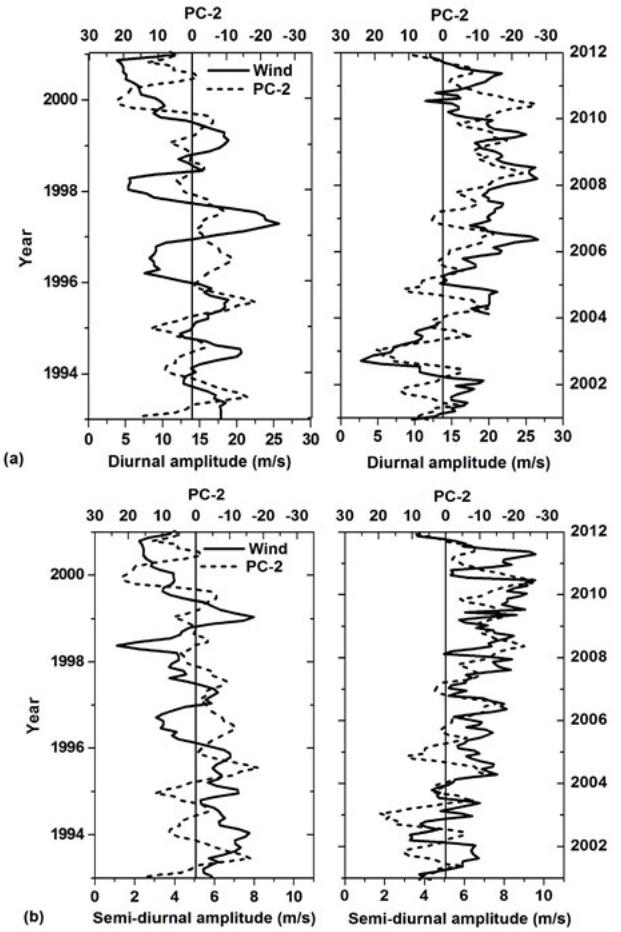

Figure 10. (a) Comparison plot for PC-2 and diurnal tide (top panel). (b) Same as (a) but for the semi-diurnal tide (bottom panel).

their values during high solar activity), the PC-2 eigen coefficient revealed negative values. The eigen coefficients were consistently negative between 2005 and 2011 and both diurnal and semi-diurnal tidal amplitudes were larger than climatological means during these times (also refer to Figure 8 for diurnal tide amplitudes). Further, when the results for the two parameters plotted in Figure 10 were broken into 3-year segments and a correlation analysis performed, a higher correlation (correlation coefficient between 0.5 and 0.9) was obtained for the descending phase of the solar cycle (2002-2008). The correlation during the ascending phase (1996-2001), was, however, negligible or weak.

CONCLUDING REMARKS

With nineteen years of observational data, the present work has demonstrated the utility of the MNOC technique in the analysis of EEJ and its long-term variabilities. The dominant principal components revealed by this technique have very close association with the diurnal range in EEJ and higher order field variation like the CEJ. Availability of MF radar observed winds enabled us to examine the upper mesospheric tidal winds and their variabilities. An important finding of this work has been the enhanced tidal activity during the solar minimum years of 2005-2010, which was likely to be driving the frequent CEJs during this period.

In contrast to the numerical modelling results of Yamazaki et al. (*2014a*), though the semi-annual variation in EEJ is quite regular, the occasional bursts of tidal activity noticed in MF radar observations that modulate the semi-annual variation in tides may not be associated with EEJ. Two issues are needed to be addressed, when one carries out such a comparative analysis: Why do the observed winds confine to lower altitudes of ~85 km, while the EEJ current flows much higher above (~105 km)?Another issue is that it is not known what fraction of the observed tidal wind field is global and what fraction is contributed by local winds. Winds averaged over several days are expected to be of global in origin but this presumption is yet to be tested with satellite data or by other means. It is indeed puzzling that low latitude mesospheric tides show a better correlation with higher order field variation like the CEJ but correlate poorly with the regular diurnal variation in EEJ. This will form

a subject matter of further investigation. It is also to be noted that some of the afternoon CEJs were likely to be caused by the disturbance dynamo effects that were not fully removed in the analysis.

ACKNOWLEDGEMENTS

Authors thank the reviewers for critical evaluation and useful suggestions in improving the quality of the manuscript.

REFFERENCES

Alex, S., Kadam, B.D. and Rao, D.R.K., 1998. Ionospheric current systems on days of low equatorial ΔH, J. Atmos. Solar-Terr. Phys., v.60, pp:371-379.

Bhargava, B.N. and Sastri, N.S., 1977. A comparison of days with and without occurrence of counter-electrojet afternoon events in the Indian region, Ann. Geophys., v.33, pp:329-332.

Bhargava, B.N., Arora, B.R. and N.S. Sastri, 1983. Indices of equatorial electrojet and counter-electrojet in the Indian region: Evolution of the indices and their authenticity, Proc. Indian Acad. Sci., v.92, pp:45-55.

Campbell, W.H., Schiffmacher, E.R. and Arora, B.R., 1992. Quiet geomagnetic field representation for all days and latitudes, J. Geomag. Geoelectr., v.44, pp:459-480.

Chapman,S. and Bartels, J., 1940. Geomagnetism, Oxford University Press.

Chen, G.X., Xu, W.Y., Du, A.M., Wu, Y.Y., Chen, B. and Liu, X.C., 2007. Statistical characteristics of the day-to-day variability in the geomagnetic Sq field, J. Geophys. Res., v.112, A06320, doi:10.1029/2006JA012059.

De Michelis, P., Tozzi, R. and Cousolini, 2010. Principal components' features of mid-latitude geomagnetic daily variation, Ann. Geophys., v.28, pp:2213-2226.

Golovkov, V.P., Papitashvili, N.E., Tyupkin, Y.S. and Kharin, E.P., 1978. Division of variations of geomagnetic field on a quiet and disturbed components by a method of natural orthogonal components, Geomag. Aeron., v.18, p:511-515.

Gurubaran, S., 2002. The equatorial counter electrojet: Part of a worldwide current system? Geophys. Res., Lett., v.29, doi:10.1029/2001GL014519.

Hanuise, C., Mazaudier, C., Vila, P., Blanc, M. and Crochet, M., 1983. Global dynamo simulation of ionospheric currents and their connection with the equatorial electrojet and counter electrojet: A case study, J. Geophys. Res., v.88, p:253-270.

Kane, R.P., 1976. Geomagnetic field variations, Space Sci. Rev., v.18, pp:413-540.

Malin, S.R.C. and Gupta, J.C., 1977. The Sq current system during the International Geophysical Year, Geophys. J. R. Astr. Soc., v.49, pp:515-529.

Marriott, R.T., Richmond, A.D. and Venkateswaran, S.V., 1979. The quiet time equatorial electrojet and counter electrojet, J. Geomag. Geoelectr., v.31, pp:311-340.

Matsushita, S., Solar quiet and lunar daily variation fields, 1967. In Physics of Geomagnetic Phenomena, Ed. Matsushita, S. and Campbell, W.H., Academic Press.

Matsushita, S. and Maeda, H., 1965. On the geomagnetic solar quiet daily variation field during the IGY, J. Geophys. Res., v.70, pp:2535-2558.

Mayaud, P.N., 1977. The equatorial counter electrojet – a review of its geomagnetic aspects, J. Atmos. Terr. Phys., 39, 1055-1070.

Onwumechili, C.A., 1977. The equatorial electrojet, Gordon and Breach Science Publishers, 627pp.

Raghavarao, R. and Anandarao, B.G., 1987. Equatorial electrojet and counter-electrojet, Indian J. Radio & Space Phys., v.16, pp:54-75.

Rajaram, M., 1980. Method of natural orthogonal components applied to equatorial geomagnetic variations, Ann. Geophys., v.36, pp:599-603.

Rajaram, M., 1983. Determination of the latitude of Sq focus and its relation to the electrojet variations, J. Atmos. Terr. Phys., v.45, pp:573-578.

Rajaram, R. and Gurubaran, S., 1998. Seasonal variabilities of low latitude mesospheric winds, Ann. Geophys., v.16, pp:197-204.

Rastogi, R.G., 1974. Westward equatorial electrojet during daytime hours, J. Geophys. Res., v.79, pp:1503-1512.

Rastogi, R.G, 1993. Complexities of ionospheric current system at low latitudes, Ann. Geophys., v.11, pp:273-282.

Rastogi, R.G., 1994. Ionospheric current system associated with the equatorial counterelectrojet, J. Geophys. Res., v.99, pp:13,209-13,217.

Richmond, A.D., 1995. The ionospheric wind dynamo: Effects of its coupling with different atmospheric regions, In the Upper Mesosphere and Lower Thermosphere: A review of Experiment and Theory, Geophys. Monogr., v.87, pp:49-65.

Richmond, A.D., S. Matsushita and J.D. Tarpley, 1976. On the production mechanism of electric currents and fields in the ionosphere, J. Geophys. Res., v.81, pp:547-555.

Sathishkumar, S. and Sridharan, S., 2013. Lunar and solar tidal variabilities in the mesospheric winds and EEJ strength over Tirunelveli (8.7°N, 77.8°E) during the 2009 major stratospheric warming, J. Geophys. Res. Space Phys., v. 118, pp. 533-541, doi:10.1029/2012JA018236.

Sridharan., S., Sathishkumar, S. and Gurubaran, S., 2009. Variabilities of mesospheric tides and equatorial electrojet strength during major stratospheric warming events, Ann. Geophys., v.27, pp:4125-4130.

Sridharan, S., Tsuda, T. and Gurubaran, S., 2010. Long-term tendencies in the mesosphere/lower thermosphere mean winds and tides as observed by medium-frequency radar at Tirunelveli (8.7°N, 77.8°E), J. Geophys. Res., v.115, doi:10.1029/2008JD011609.

Stening, R.J., 1977a. Ionospheric dynamo calculations with

semidiurnal winds, Planet. Space Sci., v.25, pp:1075-1080.

Stening, R.J., 1977b. Magnetic variations at other latitudes during reverse equatorial electrojet, J. Atmos. Terr. Phys., v.39, pp:1071-1077.

Stening, R.J., 1989. A diurnal modulation of the lunar tide in the upper atmosphere, Geophys. Res. Lett., v.16, pp:307-310.

Stening, R.J. and Winch, D.E., 1979. Seasonal changes in the global lunar geomagnetic variation, J. Atmos. Terr. Phys., v.41, pp:311-324.

Suzuki, A., 1979. UT and day-to-day variations in equivalent current systems for world geomagnetic variation, J. Atmos. Terr. Phys., v.41, pp:311-324.

Takeda, M., 1990. Geomagnetic field variation and the equivalent current system generated by an ionospheric dynamo at the solstice, J. Atmos. Terr. Phys., v.52, pp:59-67.

Takeda, M., 1999. Time variation of global geomagnetic Sq field in 1964 and 1980, J. Atmos. Solar-Terr. Phys., v.61, pp:765-774.

Takeda, M. and Maeda, H., 1981. Three-dimensional structure of ionospheric currents, 2. Currents caused by diurnal tidal winds, J. Geophys. Res., v.86, pp:5861-5867.

Tarpley, J.D., 1970a. The ionospheric wind dynamo, I, Lunar Tides, Planet. Space Sci., v.18, pp:1075-1090.

Tarpley, J.D., 1970b. The ionospheric wind dynamo, II, Solar Tides, Planet. Space Sci., v.18, pp:1091-1103.

Tarpley, J.D., 1973. Seasonal movement of the Sq current foci and related effects in the equatorial electrojet, J. Atmos. Terr. Phys., v.35, 1063-1071.

Xu, W.-Y and Kamide, Y., 2004. Decomposition of daily geomagnetic variations by using method of natural orthogonal component, J. Geophys. Res., v.109, A05218, doi:10.1029/2003JA010216.

Yamazaki, Y.,, Richmond, A.D., Maute, A., Wu, Q., Ortland, D.A., Yoshikawa, A., Adimula, I.A., Rabiu, B., Kunitake, M. and Tsugawa, T., 2014a. Ground magnetic effects of the equatorial electrojet simulated by the TIE-GCM driven by TIMED satellite data, J. Geophys. Res., v.119, pp:3150-3161, doi:10.1002/2013JA019487.

Yamazaki, Y., Richmond, A.D., Maute, A., Liu, H., Pedatella, N. and Sassi, F., 2014b. On the day-to-day variation of the equatorial electrojet during quiet periods, J. Geophys. Res., v.119, pp:6966-6980, doi:10.1002/2014JA020243.

Yamazaki, Y., Yumoto, K., Uozumi, T., Abe, S., Cardinal, M.G.C., Mcnamara, D.J., Marshall, R., Shevtsov, B.M. and Solovyev, S.I., 2010. Reexamination of the Sq-EEJ relationship based on extended magnetometer networks in the east Asian region, J. Geophys. Res., v.115, doi:10.1029/2010JA015339.